International Journal of Emerging Research Frontiers (IJERF)

Volume 1, Issue 1, January – March (2026)

Local Tone Mapping Operator based on Layer Decomposition

Qiumei[1], Chuanjie Li[2]

National Professional Laboratory of Color Science and Engineering, School of Optoelectronics, Beijing Institute of Technology, Beijing 100081, China

RESEARCH ARTICLE

Received: 10-10-2025 Revised:19-11-2025 Accepted:18-02-2026 Published:20-03-2026

Abstract— The amount of levels that a picture can support is directly determined by its dynamic range. A dynamic range of 256 is often utilised. The display device that the picture will be presented on must be taken into account when defining the dynamic range of an image. A dynamic range is considered large dynamic range if it exceeds 256. This range might go as high as 10,000. Display devices are unable to display this type of picture.

This is unable to distinguish between a lot of visual information. In order for the standard display units to adapt the format, this type of visual information must be translated. This needs to be completed with little information loss. Several tone mapping operators carry out this really important task. There are two kinds of tone mapping operators: local and global. The same mapping function is applied throughout the picture using global tone mapping operators, whereas local tone mapping

For local areas of the picture, operators employ several mapping functions. Despite the improved quality of global TMOs, the converted picture has several halo effects. To lessen these consequences, a global TMO based on decomposition is presented in this study. The image is broken down into two layers: base and detail. To enhance the quality of the transformed picture, a hybrid decomposition and optimisation are suggested.

Index Terms— base layer, detail layer, retinex decomposition, TMQI, Tone mapping

1 INTRODUCTION

Finite ranges of visual information are often captured by image capture systems. Large amounts of memory and processing power are needed to handle the original continuous visual data. Rather, the feasible capturing devices only record limited levels, which reduces the amount of memory and processing power required. The endless visual data is reduced and lost in the process. For standard dynamic range (SDR) picture capture equipment, this is the situation. Low dynamic range (LDR) photos are another name for SDR images. On the other hand, high dynamic range picture capture systems collect as much visual information as possible, but not all of it.

A raw file is created from the HDR-captured picture. Regardless of storage and display issues, all of the information is included in this raw file. The raw picture is retrieved at the display unit's output if we look at a particular display unit. Tone mapping is the process of converting HDR to LDR or SDR. Tone mapping operators are those who perform this. The primary function is to convert high dynamic range images into low dynamic range and get the output picture without any data loss from the source image. In order to present the HDR photographs at the output, the tonal values are changed.Global TMOs and local TMOs are the two categories into which the TMOs are divided. Reinhard and Gamma correction TMOs are the most often used TMOs. We only take into account one relative function in the Global TMOs. The quantity of important information would be lost if just one curve were taken into account for the whole picture. To counteract the information loss, we take into account a curve in the local TMOs for each block. In the case of a global tone mapping operator, the pixels are identical when we examine the relationship between the raw data and the mapped picture. This brings us to the overall picture consideration: some data will be lost when the visualization has a variety of backgrounds, objects, and appearances. This method is easier to build and executes more quickly [1]–[3].
A separate relation is used when mapping pixels to a raw file using the local tone mapping operator. The image's brightest and darkest points are referred to as the dynamic range [4]–[6].

2 GAMMA CORRECTION

2.1 Introduction

To show a picture flawlessly on a computer screen, gamma correction is used. Gamma correction regulates an image's overall brightness. Gamma correction is used to adjust the brightness of a picture that may be damaged or dark. In addition to brightness, the different ratios of red, blue, and green are also adjusted. The manufacturer simply takes into account the intensity to voltage response, regardless of the kind of computer monitor. The intensity to voltage response for every computer monitor varies about up to 2.5 power functions. Let's look at an example where we transmit a picture to the monitor's input and a specific pixel has an intensity of x. The monitor's output is thus specified as x^2.5. However, the monitor's voltage reading falls between 0 and 1. Thus, we can determine that the monitor's output value falls below 2.5. Thus, the gamma correction is used to modify the image's brightness. Every monitor in real-world applications has to function similarly to the gamma corrector [7]. The definition of the power law equation for a gamma correction is the

$$V_{out}=A.V_{in}^{\gamma}$$

Here we can get the output by the product of a constant with the input voltage.

Here A can either be 0 or 1. if gamma value less than 1 it is called encoding gamma and called as gamma compression [8].

If the gamma value greater than 1 it is called decoding gamma and called as gamma expansion. The gamma concept can be used at any nonlinear devices like cathode ray tubes. When the above equation is converted into logarithmic form then it can be defined as follows:

$$\gamma=d\log(V_{out})/d\log(V_{in})$$

Its application can be found in film photography and CRTs. The characteristic curve of a photo film is defined as

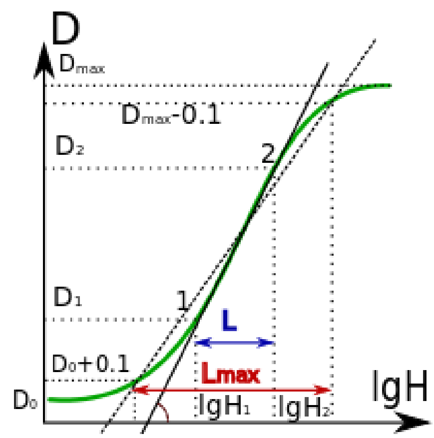

Fig. 1 Photo Film Characterization

2.2 Color Correction

It is a methodical procedure used in filmmaking, television, stage lighting, and other fields. Color gels or filters are used to change the light's overall color. Color temperature is a scale used to quantify the color of light. The picture or video may have a range of colors if the color gels are not applied. The color of the light sources may be changed by applying color gels in front of them. When it is shown on a television or in a movie theater, mismatched lighting might create an undesirable aesthetic [9].

Conversely, these color gels are mostly used in tint lights for artistic impact and motivated lighting. It is a technological procedure that resolves color problems and improves the image's naturalness. Making the picture as clear as feasible for human vision in the actual world is the primary goal of color correction. The word itself implies fixing color problems by making black look black, white appear white, and even more natural. Photoshop is the primary application for it. It is a program that may be used to alter and modify photos, make a clipped route, and get the required image. Parts of a picture may be matched, altered, or corrected using a variety of techniques. We separate the color picture into three components—brightness, contrast, and color balancing—to make the procedure easier.

International Journal of Emerging Research Frontiers (IJERF)

Volume 1, Issue 1, January – March (2026)

right away, it seems black or even dark. Therefore, we need to fill that region in the 16 bits in order to get around this. In order to make the picture surface black, the next stage in the process is to establish black for the point of reference as the highest relative values of RGB channels in an RGB image. The picture that is now seen is completely dark. This stage allows us to identify an image's saturated pixels. Curve modifications allow us to make the image seem more realistic to the unaided eye.

3 Retinex-based Decomposition

A The basic retinex model of an image is given below.

$$S = R.L$$

where S is the original image, R is reflectance and L is illumination. The retinex theory was developed in 1971 by Land and McCann [11], is used as a fundamental theory in many core image processing schemes. The problem of intrinsic images is stated as follows:

Given an image $I : H \times \{1,\dots,H\} \times W \rightarrow 255^3$ with N=HW and a set of images $I_1,\dots,I_T$ or a video $V : H \times W \times T \rightarrow 255^3$ with N=HWT, estimate the respective reflectance image **R** and shading image **S** for each image. The above stated problem is originally stated by Barrow and Tenenbaum [12]. Land and McCann [11] introduced the retinex theory with an assumption of Mondrian world. A painting of Dutch painter Mondrian is shown in Fig. 1 along with the reflectance computation by Land and McCann [11]. The intuition behind the theory of Retinex is stated as follows.

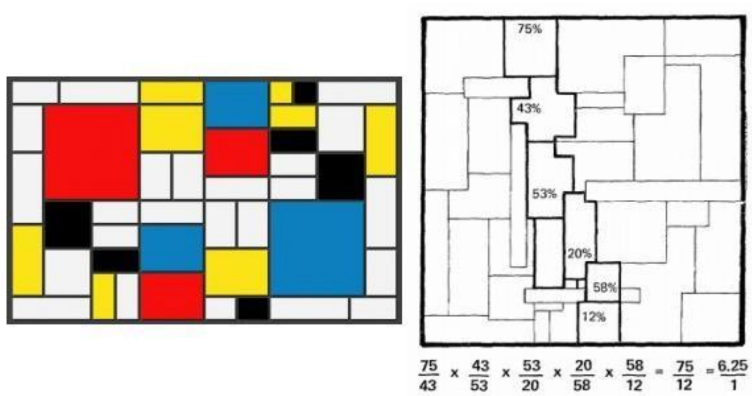

Fig. 2 Mondrian painting and the reflectance computation by Land and McCann [13]

Along the path, multiply the measured intensity ratios. These mechanisms are later formalized [14] and extended to color images [15]. The reflectance of each pixel in the channel I is calculated by building a family $\{x_k\}_{k=1}^{K_j} \subset H \times W$ of **J** paths. The reflectance $R_c(x_c)$ of pixel x_n in the channel **C** is calculated as follows.

$$R_C(x_{nC}) = \frac{1}{J}\sum_{j=1}^{J}\sum_{k=1}^{K_j} \delta\left(I_C(x_k) - I_C(x_{k+1})\right)$$

where

$$\delta(x) = \begin{cases} |x| & if\ |x| > \varepsilon \\ 0 & otherwise \end{cases}$$

The problem of this method is to choose the paths $\{x_k\}_{k=1}^{K_j}$ so that the above equation can calculate the reflectance accurately.

4 L0-L1 Layer Decomposition

The optimization is given by

$$\min_{S,B} \sum_{p=1}^{N} \left((S_p - B_p)^2 + \lambda_1 \sum_{i \in \{x,y\}} \left|\partial_i B_p\right| + \lambda_2 \sum_{i \in \{x,y\}} F(\partial_i B_p) \right)$$

International Journal of Emerging Research Frontiers (IJERF)

Volume 1, Issue 1, January – March (2026)

Here the pixel is indexed by p and the total number of pixels is N. The optimization model contains three terms. The first term in the expression $\sum_i \sum_p \left(S_p - B_p\right)^2$ enforces the difference between the base layer original image to be very less. The second term $\left|\nabla B\right|$ is an ℓ_1 gradient sparsity term which includes the partial derivative. The third term express the structural property of detail layer. It is expressed as an ℓ_0 gradient sparsity stretch. The term includes a representing function F(x) which is unity for x≠0 and zero for x=0.

The above objective function is non-convex. This is because of ℓ_0 regularization component contained in the third term. An irregular direction scheme of multipliers is presented to resolve this problem. The objective function is rewritten below with matrix terms.

$$\min_b \left\{ \frac{1}{2}\left\| s - b \right\|_2^2 + \alpha \left\| \nabla b \right\|_1 + \beta\, 1^T F\left(\nabla (s - b)\right) \right\}$$

Here s and b belong to $\mathbb{R}^N$ which are concatenated versions of ***S*** and ***B***. ∇ denotes a combination of multiple gradient operations given as

$$\nabla = \left[\nabla_x^T, \nabla_y^T\right]^T \in \mathbb{R}^{2N \times N}$$

The ***F*** function performs elementwise non-zero indication. The resulting Lagrangian function is given below.

S = 0.01380, N = 0.432760 and Q = 0.54210 S = 0.01250, N = 0.268130 and Q = 0.52680

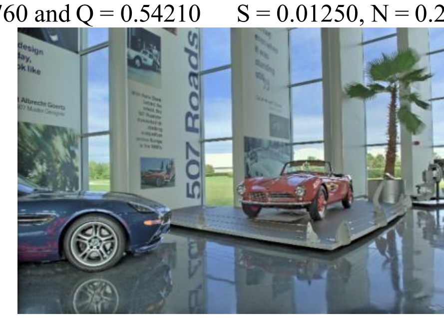

S = 0.01320, N = 0.695560 and Q = 0.53510 S = 0.01220, N = 0.488250 and Q = 0.52250

S = 0.05370, N = 0.350450 and Q = 0.82090 S = 0.01380, N = 0.432760 and Q = 0.73130

International Journal of Emerging Research Frontiers (IJERF)

Volume 1, Issue 1, January – March (2026)

S = 0.05170, N = 0.508780 and Q = 0.81130

S = 0.05600, N = 0.923540 and Q = 0.83140

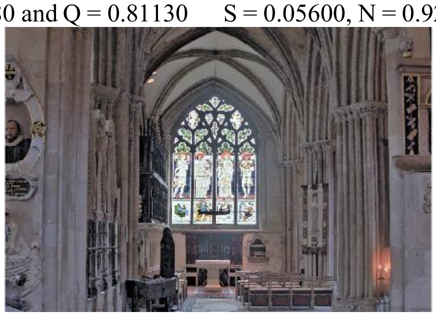

S = 0.01380, N = 0.153160 and Q = 0.54250

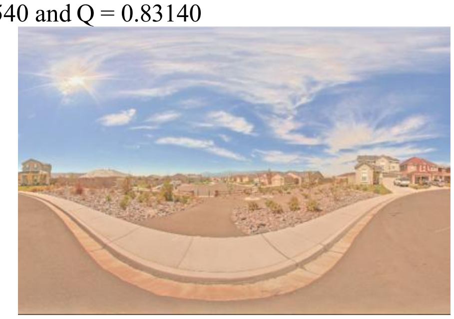

S = 0.05610, N = 0.652790 and Q = 0.83160

Fig. 3 Simulation Results using the proposed Tone Mapping

where y_i are Lagranian dual variables. The quadratic programming problem which will be resulted by splitting c_1^k, c_2^k, y_1^k and y_2^k can be solved using FFT effectively. When this $\ell_1 - \ell_0$ decomposition is applied to the radiance map, a piecewise smooth base and constant detail layers can be obtained.

5 Results and Discussions

Simulation results and performance comparison of the proposed technique are discussed in this section. The denoising, deblurring and compression operations are widely used. Tone mapping is widely used in image processing operations and it does not contain any reference image. In 2013, H. Yeganeh and Z. Wang proposed an objective quality assessment in the form of Tone Mapped image Quality Index (TMQI) [16][17]. This parameter balances the importance of two existing objective measures. They are Structural fidelity (S) and Naturalness (N). The structural fidelity is defined as follows.

$$S = \prod_{l=1}^{L} S_l^{\beta_l}$$

Here L is the number of scales and β_l is the weight for l^{th} scale. The structural fidelity is defined by dividing the image into patches.

The local fidelity S_l is defined by the following relation where x and y are the respective patches from HDR and tone-mapped images [18]-[21].

Here σ_x, σ_y and σ_{xy} are the auto and cross correlations. C_1 and C_2 are the positive stabilizing constants. Naturalness is basically a subjective measure; but a quantitative analysis is presented for this parameter. Histograms of mean and deviations are the measures of intensity and contrast. Correspondingly, the Naturalness is defined as

$$N = \frac{1}{K} P_m P_d$$

Here K is a normalization factor given by K = max $\{P_m\ P_d\}$. P_m and P_d are the density functions of mean and deviation respectively. The TMQI is defined in terms of these two parameters as follows.

$$TMQI = aS^{\alpha} + (1 - a)N^{\beta}$$

The Fig. 3 shows the tone mapped image along with the objective measures.

6 Conclusions

The division of an input picture into basic and detail layers is referred to in the project description as a layer decomposition. The primary use of this technology is picture restoration. In contrast, this method keeps a lot

International Journal of Emerging Research Frontiers (IJERF)

Volume 1, Issue 1, January – March (2026)

of valuable information in the original picture. The halo effect and over-enhancement effect have been addressed in the Global TMOs. While the spatial structure has grown in the detail layer, the dynamic range has decreased in the base layer. These are the typical shortcomings of global tone mapping that can be addressed by these multitone mapping techniques, and multitone mapping has high visual quality. The technique used on a few photos shown that they are deserving of excellent quality.

REFERENCES

[1] K. Devlin and E. Reinhard. Photoreceptor physiology serves as an inspiration for dynamic range reduction. IEEE Transactions on Computer Graphics & Visualization, 11(1):13–24, January 2005.

[2] H. Rushmeier and J. Tumblin. replication of tones for realistic pictures. IEEE Computer Graphics and Applications, November 1993, 13(6):42–48.

[3] G. Ward. A contrast-based luminance display scale factor Graphics Gems IV, pages 415–421, 1994.

[4] "An Adaptive Tone Mapping Algorithm for High Dynamic Range Images," J. Zhang and S. Kamata, Lecture Notes in Computer Science, 2009, Volume 5646/2009, 207-215.

[5] R.L. Joshi K.E. Spaulding and G.J. Woolfe, "Using a residual image formed from a clipped limited color gamut digital image to represent an extended color gamut digital image," US6301393B1, United States Patent and Trademark Office, 2000.

[6] J. Ferwerda, P. Shirley, M. Stark, and E. Reinhard. replication of photographic tones in digital photos. July 2002; ACM Trans. Graph., 21(3):267–276.

[7] J. Dorsey and F. Durand. Quick bilateral filtering for high dynamic range picture presentation. ACM Trans. Graph., 21(3), July 2002, 257–266.

[8] Y. Li, E. H. Adelson, and L. Sharan. using subband architectures to compress and expand high dynamic range photos. ACM Trans. Graph., July 2005, 24(3):836–844.

[9] S. Susstrunk and L. Meylan. Using an adaptive filter based on Retinex, high dynamic range images are rendered. IEEE Transactions on Image Processing, 15(9):2820-2830, September 2006.

[10] R. Fattal, D. Lischinski, R. Szeliski, and Z. Farbman. Decompositions that preserve edges for manipulating tone and detail on several scales. August 2008; ACM Trans. Graph., 27(3):67:1–67:10.

[11] Lightness and retinex hypothesis, E. H. Land and J. J. McCann. January 1971, Journal of the Optical Society of America, 61(1):1–11.

[12] J. M. Tenenbaum and H. G. Barrow. retrieving inherent scene features from pictures. New York, NY: Academic Press, 1978.

[13] https://davidstutz.de/retinex-theory-and-algorithm/ Last seen on April 27, 2020.

[14] Horn, B. K. P. assessing an image's brightness. December 1974, Computer Graphics and Image Processing, 3(4):277-299.

[15] A. Blake. Limitations for calculating lightness in the Mondrian universe. 32(3):314-327, Computer Vision, Graphics, and Image Processing, 1985.

[16] Hojatollah Yeganeh and Zhou Wang, "Objective Quality Assessment of Tone-Mapped Images," IEEE Transactions on Image Processing, vol. 22, No. 2, February 2013.

[17] Zhetong Liang, Jun Xu, David Zhang, Zisheng Cao, and Lei Zhang, "AHybrid l1-l0 Layer Decomposition Model for Tone Mapping," CVPR 2018.

[18] Wavelet Packet: A Multirate Adaptive Filter for Denoising of TDM Signal, V. V. Satyanarayana Tallapragada, G. V. Pradeep Kumar, and Jaya Krishna Sunkara, International Conference on Electrical, Electronics, Computers, Communication, Mechanical and Computing (EECCMC), January 28-29, 2018.

[19] "Super-Resolution Based Image Reconstruction," International Journal of Computer Science and Technology, vol. 2, Issue 3, pp. 272-281, September 2011; Jaya Krishna Sunkara, Kuruma Purnima, Suresh Muchakala, Ravisankariah Y.

[20] "Multiresolution SVD based Image Fusion," Dr. G.A.E. Satish Kumar and Jaya Krishna Sunkara, IOSR Journal of VLSI and Signal Processing, vol. 7, Issue 1, ver. 1, pp. 20-27, Jan-Feb 2017. 10.9790/4200-0701012027 is the doi.

[21] Jaya Krishna Sunkara, M Santhosh, C Suneetha, and V. V. Satyanarayana Tallapragada, "Vector Quantization –

International Journal of Emerging Research Frontiers (IJERF)
Volume 1, Issue 1, January – March (2026)

A Comprehensive Study," International Journal of Engineering Science Invention, vol. 7, Issue 5, May 2018, pp. 27-38.